Hydrodynamic-Analogy-Based Model for Efficiency of Structured Packing Columns

A. Shilkin and E. Y. Kenig
Dept. of Biochemical and Chemical Engineering, University of Dortmund, Emil-Figge-Str.70, 44227 Dortmund, Germany

Z. Olujic
Delft University of Technology, Laboratory for Process Equipment, Leeghwaterstraat 44, 2628 CA, Delft, The Netherlands

DOI 10.1002/aic.10937
Published online July 26, 2006 in Wiley InterScience (www.interscience.wiley.com).

A model based on the hydrodynamic analogy approach was developed for the prediction of temperature and composition profiles in structured packing distillation columns. Compared to the traditional models based on the film theory, the proposed model is more rigorous. It comprises Navier-Stokes equations, convection-diffusion and heat-conduction equations to describe the transport phenomena under condition of two-phase gas-liquid flow in an entire separation column. As a result, modeling the column efficiency is accomplished without application of the mass-transfer coefficients. For the model verification, total reflux distillation data for binary and multicomponent mixtures are used. Calculations with both the hydrodynamic-analogy-based, and the film model are performed for a wide range of operating conditions. The proposed model is shown to have a more stable performance than the traditional one. Therefore, it can be recommended for design, revamp and optimization of distillation columns equipped with corrugated sheet structured packings. © 2006 American Institute of Chemical Engineers *AIChE J,* 52: 3055–3066, 2006

Keywords: structured packings, hydrodynamic analogy, distillation

Introduction

Since the early 1980s, when corrugated sheet metal structured packings appeared on the market, great advances toward the process intensification in distillation and absorption have been made. Being initially developed for separation of thermally unstable components in vacuum distillation, structured packings have permanently been gaining in popularity and cover a large field of applications in chemical, petrochemical and refining industries[1] due to their more effective performance characteristics. Most commonly, at sub- and near-atmospheric pressures, structured packings outperform random packings and trays in capacity and/or separation efficiency. For instance, Kurtz et al.[2] reported that the distillation capacity can be increased by as much as 30%–50% at the same separation efficiency, when trays are replaced with structured packing.

It is widely known that structured packing performance characteristics depend heavily on the corrugation geometry. To match the ever growing demand on capacity, some 15 years ago, most manufacturers offered modified structured packings in which the corrugation inclination angle with respect to horizontal was increased from standard 45 to 60°. Performance characteristics of both conventional 45 and 60° packings were thoroughly investigated experimentally by the Separation Research Program (SRP), Fractional Research, Inc. (FRI), and the TU Delft group.[3-6] It has been found that the improved capacity of the 60° packings was largely counterbalanced by the deteriorated separation efficiency. Therefore, recent efforts have been directed toward investigation of the mechanisms contributing to the structured packings performance, using both ex-

Correspondence concerning this article should be addressed to E. Y. Kenig at e.kenig@bci.uni-dortmund.de.

periments and computational fluid dynamics (CFD).[7] These studies have brought about a new generation of structured packings on the basis of the standard high-efficiency 45° packing, with the modified bottom or top and bottom ends of each layer.[8,9] This geometry optimization resulted from the better understanding of complex interplay between the phase interactions and packing geometry, and allowed a substantial (20%–30%) gain in capacity.[6] The development of this so-called high-capacity packing represents the major breakthrough in structured packing design during the past 10 years.

An accurate model-based design of separation columns equipped with structured packings represents a challenging task, and becomes increasingly important due to the growing implementation of these packings. According to the estimate by Brunazzi and Paglianti,[10] about 25% of the refinery vacuum towers worldwide were equipped with structured packings in 1997. The modern modeling approaches are expected not only to deliver reliable results on the column hydraulic and separation characteristics, but also to fill the gaps in understanding of the mass-transfer mechanisms. Therefore, the predictive models based on physically consistent considerations become especially important. This would make it possible to properly account for hydrodynamics and transport phenomena, and to represent them as functions of the corrugation geometry and packing surface characteristics.

A number of modeling approaches for the prediction of the column hydraulic and separation performance are available in the literature. The most advanced of them are based on direct consideration of the packing corrugation geometry. An overview of main geometry-based models is given by Shilkin and Kenig.[11] In these approaches, actual rates of multicomponent mass and heat transport are taken into account directly. Most commonly, mass transfer at the gas-liquid interface is described using the film theory.[12,13] According to this theory, all the resistance to mass transfer is localized in thin films adjacent to the gas-liquid interface. Mass transfer occurs within these films solely by steady-state molecular diffusion in the direction normal to the interface. For multicomponent separations which are most commonly encountered in industrial practice, multicomponent diffusion in the films is described by the Maxwell-Stefan equations which can be derived on the basis of the kinetic gas theory.[14,15] Outside the films the level of mixing is assumed so high that no composition gradients in the bulk-fluid phases exist. Thermodynamic equilibrium is assumed only at the interface. The hydrodynamic and mass-transfer effects are taken into account by applying correlations for mass-transfer coefficients k_L, k_G for the liquid and gas phases, as well as for the holdup and pressure drop. Usually, these correlations are empirical. Along with hydrodynamic and physicochemical characteristics, such as Reynolds and Schmidt numbers, they may include explicitly different packing geometric properties.[4,16-18]

The film model is relatively simple and applicable for different types of column internals. Nevertheless, its application is not always problem-free. Due to rather limited physical representation of this model, influence of the broad spectrum of packing geometric characteristics and operating conditions is translated into empirical correlations to estimate two *imaginary stagnant* film thicknesses. Since the film model does not contain any momentum transfer equations, its accuracy depends heavily on ability of the employed correlations to account for changes in the flow conditions, due to different packing geometry and fluid physical properties. Considering that these correlations are usually determined experimentally for a certain packing, chemical system, and within a definite range of operating conditions, their extrapolation to other conditions is inherently risky.

Further difficulties arise when the film theory is applied to complex multicomponent and reactive separations. Being developed for a binary mass transfer,[12] this theory directly relates the film thickness with the binary diffusivity. However, in a multicomponent mixture, different diffusivities related to different component binary pairs are available, which result into several thicknesses. To obtain the only film thickness for each phase, this model parameter has to be estimated as an averaged value. Moreover, in reactive systems, the film thickness should also depend on the reaction rates. This dependence cannot, however, be reflected by the model. A formal contradiction is often related to the consideration of convective mass transfer by the film theory, since the main elements of this model represent stagnant films.

Nowadays, the film model is used for much more complicated processes, than those considered in the original study.[12] This requires additional assumptions, which are frequently in conflict with the physical backgrounds. As a consequence, the straightforward application of the film model becomes difficult.

The objective of this work is to present an alternative way for the description of the mass-transfer efficiency of separation columns equipped with structured packings, based on the hydrodynamic analogy approach,[19] and more specifically, on the model reported recently by Shilkin and Kenig.[11] This model is extended here to improve the accuracy for higher gas loads by directly incorporating the gas-phase turbulence. The proposed model has been verified against experimental data on distillation of binary and ternary mixtures in columns equipped with different types of structured packings.

Hydrodynamic Analogy Approach

The hydrodynamics, heat and mass transfer in separation columns can be rigorously described by the partial differential equations governing momentum, energy and mass transport (Navier-Stokes, convection-diffusion and heat conduction equations). These equations should be supplemented by the appropriate boundary conditions at the phase boundaries. In the case of geometrically simple flow patterns, as, for instance, planar films, spherical drops, and so on, their boundaries can be exactly localized, and, thus, for these simple geometries, the heat and mass transfer can be described on a purely theoretical basis, without application of any adjustable parameters.[20]

However, the majority of industrial separation processes occur under extremely complicated flow conditions, and, thus, exact localization of the phase boundaries is hardly possible. The real hydrodynamics is, therefore, replaced by a simplified one, whereas the film or other similar model is usually applied. To describe real conditions, the necessary model parameters have to be estimated experimentally.

Hydrodynamic analogy approach is an alternative way to describe the hydrodynamics and transport phenomena in processes in which the exact location of the phase boundaries is not possible. The basic idea of the approach is a reasonable *replacement* of the actual complex hydrodynamics in a column

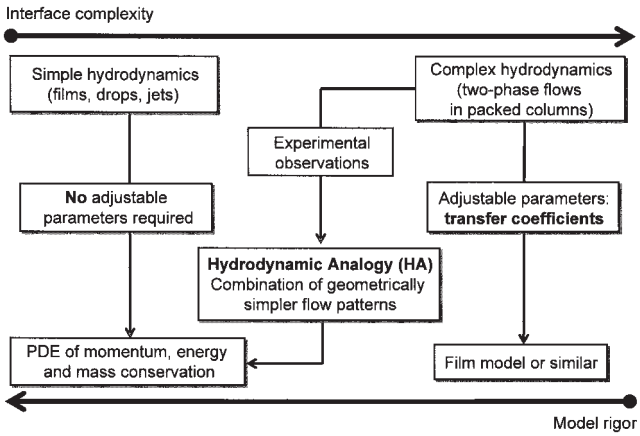

Figure 1. Modeling approaches.

by a combination of *geometrically simpler flow patterns* (see Figure 1). Such a geometry simplification has to be done in agreement with *experimental observations* of fluid flow, which plays a crucial part for the successful application of this approach. Once the observed complex flow is reproduced by a sequence of the simplified flow patterns, the partial differential equations of momentum, energy and mass transfer are applied to describe the transport phenomena in an entire separation column.

Fluid Dynamics in Structured Packings

Corrugated sheets structured packings are installed in a column in the form of beds of certain height and diameter. The beds consist of layers (segments) of approximately 200 mm height, with each subsequent layer rotated usually by 90° with respect to the preceding one to promote lateral spreading of the liquid in all directions. The structured packing layers are composed of a number of corrugated sheets manufactured from gauze, metal, ceramics or plastics. The surface of the corrugated sheets, usually provided with a regular pattern of holes, can be additionally treated mechanically or chemically to promote liquid spreading and to enlarge gas-liquid interfacial area. The corrugation inclination angle is reversed in adjacent sheets which results into a "toblerone-like" structure,[21] with the alternatively oriented flow channels.

Liquid flow

The main purpose of corrugated sheet structured packings is to ensure continuous thin film flow providing well developed interfacial area between liquid and gas flows in channels.[17] In reality, the liquid flow over the packing surface depends in an intricate way on the liquid and surface characteristics, corrugation geometry and operating conditions. To understand the influence of these factors on the liquid-flow behavior is essential for an accurate prediction of the packing mass-transfer efficiency, especially when the resistance to mass transfer is mainly located in the liquid phase (for example, in absorption of CO_2).

Investigations of liquid flow over the structured packings, both experimentally and by means of CFD, have been a subject of considerable interest during the last years.[22-25] It has been shown that for a wide spectrum of flow rates, the liquid flow paths remain the same, thus, being independent of inertial effects (except for the packings with sharp corrugation ridges), and follow the minimal angle with respect to vertical (the so-called gravity or effective flow angle).[26] The observed liquid-flow path is sketched in Figure 2. The mixing points are related to the corrugation ridges, where the film flow structure is disturbed due to the abrupt change in the flow direction and influence of intersection points with adjacent corrugated sheets.

Depending on both liquid and gas flow rates, as well as on the packing geometric and surface characteristics, the form of liquid flow may vary from laminar films with constant thicknesses to rivulets. Since the best structured packing separation efficiency is achieved under conditions of stable film flow, in engineering practice, the packing characteristics are determined to ensure just this flow type.

Gas flow

The countercourse assemblage of the corrugated sheets in a packing layer (see Figure 3) results into a set of channels with identical cross section and alternating ($-\varphi$ and φ) inclinations with respect to the column axis. The lengths of individual channels depend on the packing layer height L, and the corrugation inclination, φ. Channels ending at the column walls are generally shorter than those in the bulk of the packing. According to the observations,[27] gas flow takes place in the channels in the direction dictated by the corrugation inclinations. Each channel is formed by two wall sides s_0 and one open side b_0, which faces a neighboring channel, and is shared between these two adjacent channels (see Figure 3c).

Dissipation mechanisms responsible for the pressure drop in structured packings have been studied experimentally by Olujić[17] who distinguished between the following three major components:

1. Gas-liquid interfacial friction,
2. Gas-gas friction at the open channel side between the two adjacent channels (cf. Figure 3c),

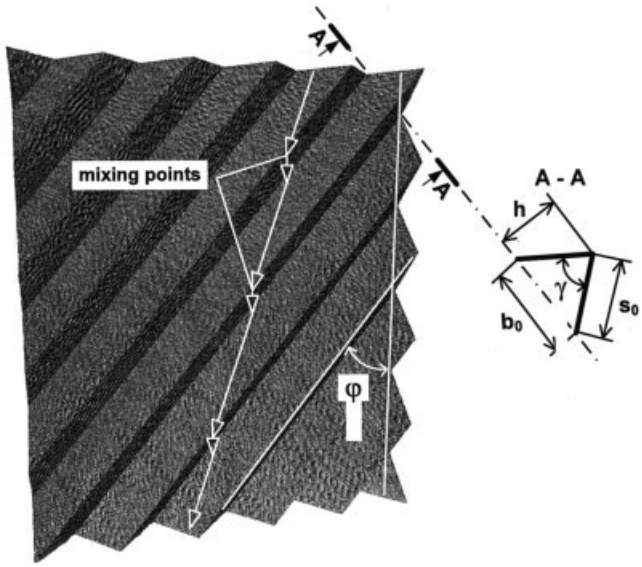

Figure 2. Corrugation geometry and observed liquid flow path.

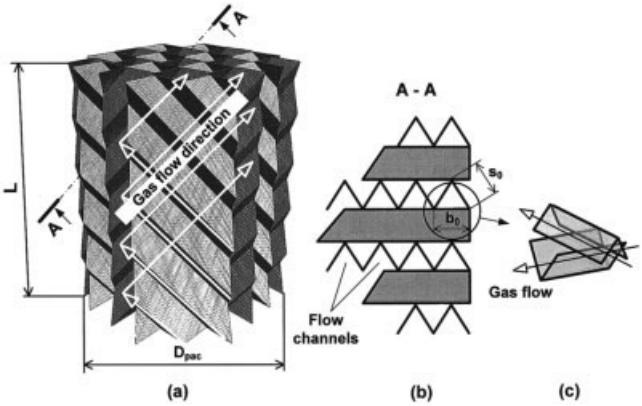

Figure 3. Gas flow through a packing layer (a), sectional view (b), adjacent gas flow channels (cross-over) (c)

3. Abrupt flow redirection at the column wall and at the transitions between the packing layers.

Recently, Petre et al.[28] performed a comprehensive CFD-based study on the impact of different dissipation mechanisms on the total pressure drop under conditions of a single-phase gas flow. It has been shown that the most dominant part (60 to 80%) is contributed by the gas-gas friction at the open-channel side, following by form drag at the transitions between the packing layers and at the column wall. Similar results have been obtained by Egorov et al.[29]

Although the contribution of each dissipation mechanism to the dry pressure drop in structured packings is well investigated, their influence on the mass transfer still remains unclear. The reason is that the gas-liquid phase interactions are very complicated, especially if the conditions near and above the loading point are considered. Therefore, direct CFD simulations of such complex two-phase flows accompanied by the heat and mass transfer appear unrealistic in the near future.[30] As a consequence, the influence of each mechanism on the packing mass-transfer efficiency is estimated empirically. For instance, an experimental study performed by Olujić[17] led to the assumption that only the gas-liquid friction at the phase interface enhances the mass transfer substantially. The other mechanisms were found irrelevant, thus producing just the "useless" pressure loss. This is particularly important with regard to the gas-gas friction (mechanism 2), which, according to Stoter et al.,[24] is responsible for local, that is, small-scale gas flow mixing. Based on this assumption, some attempts to eliminate the gas-gas friction at the open-channel side have been done, by introducing thin flat sheets between the corrugated sheets in order to isolate the channels.[31,32] By adopting this so-called monolith-like structure with a set of closed inclined channels, a considerable reduction of the total pressure drop has been anticipated. At the same time, replacement of the gas-gas friction "useless" for the mass transfer by the "useful" gas-liquid friction at the surface of the isolating sheets was expected to increase the packing separation efficiency.

The experimental investigations of the monolith-like structured packing hydraulic characteristics proved the expected pressure drop reduction accompanied by a significant capacity enhancement, despite the substantially increased geometric (installed) specific packing area due to inserted sheets.[32] The total reflux distillation experiments showed, contrary to the expectations, a rather poor separation efficiency in the preloading region. In the loading region, under all investigated operation conditions, the best achieved separation efficiency was not better than that of standard structured packings, although the geometric specific area of the modified packing was considerably larger. Such a behavior was explained by a severe liquid maldistribution, which, especially in the preloading region, appeared to be highly detrimental to the packing mass transfer efficiency.[32] The pronounced efficiency drop, while eliminating the gas-gas friction, may also indicate that the effect of this mechanism on the mass transfer was underestimated. Hence, it should be accounted for in the model development.

Model Development

Physical model

In line with the hydrodynamic analogy concept, the basis for the physical model is provided by the observations of fluid-flow together with the geometric characteristics of structured packing. The observations given in the previous section can be summarized as follows:

1. Gas flow takes place in channels built up by the countercourse assemblage of the corrugated sheets;[17,33]
2. There is a strong interaction between the gas flows in adjacent channels through the open channel side (Figure 3c), responsible for small-scale mixing (that is, via turbulence) of the gas phase;
3. Liquid generally tends to flow in form of films over the packing surface, while the wave formation is largely suppressed due to the corrugations;[23,25]
4. Liquid flows at the minimal angle built by the packing surface and the vertical axis (the so-called gravity-flow angle);[26]
5. Abrupt flow redirection at the corrugation ridges together with the influence of intersection points with the adjacent corrugated sheets cause mixing and lateral spreading of the liquid phase;[32]
6. Side-effects (abrupt flow redirection at the column wall and at transitions between the packing layers) result into large-scale mixing of the gas phase.

The physical model represented in Figure 4 comprises all these effects. The pronounced channel flow of the gas phase makes possible to consider the packing as a bundle of parallel inclined channels with identical cross sections. For simplicity, the circular channel shape is adopted. The number of the channels, as well as their diameter is determined from the packing geometric specific area and corrugation geometry, respectively. The gas-flow behavior depends on the operating conditions and varies from laminar to turbulent flow. The liquid flows countercurrently to the gas flow in form of laminar nonwavy films over the inner surface of the channels. Additionally, a uniform distribution of the both phases in radial direction is assumed, that is, no maldistribution is taken into account in the model. The ratio of wetted to total number of channels is the same as the ratio of effective (interfacial) specific area to geometric specific area of the packing

$$\frac{n_w}{n_t} = \frac{a_e}{a_t} \tag{1}$$

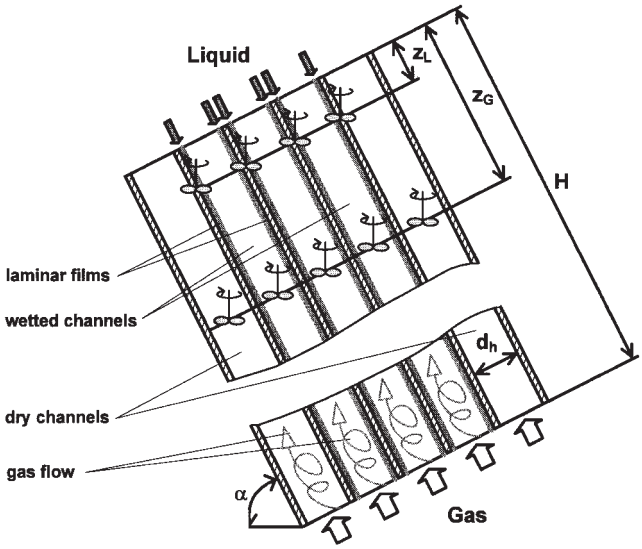

Figure 4. Physical model of structured packing.

The channels are inclined at the gravity-flow angle α to satisfy the observation 4. The large-scale mixing of the both phases caused by the abrupt flow redirection and redistribution (see observations 5 and 6) is approximated by a periodic ideal mixing. Length of the undisturbed liquid flow z_L is set to be equal to the distance between the two neighboring corrugation ridges (see Figure 2), whereas for the gas flow, z_G is calculated as an average length of all channels in a packing layer.[11]

Mathematical Model

Hydrodynamics

The liquid flow is described by the system of Navier-Stokes equations in the film-flow approximation[34]

$$\frac{1}{r}\frac{\partial}{\partial r}\left(r\mu_L\frac{\partial u_L}{\partial r}\right) - \frac{\partial P_L}{\partial x} + \rho_L g\,\sin\alpha = 0 \tag{2}$$

$$\frac{\partial P_L}{\partial r} = 0$$

whereas for the description of the gas phase, the Boussinesq approximation is adopted

$$\frac{1}{r}\frac{\partial}{\partial r}\left(r\tilde{\mu}_G\frac{\partial u_G}{\partial r}\right) - \frac{\partial P_G}{\partial x} + \rho_G g\,\sin\alpha = 0, \quad \tilde{\mu}_G = \mu_G^{lam} + \mu_G^{turb} \tag{3}$$

$$\frac{\partial P_G}{\partial r} = 0$$

The boundary conditions (see Figure 5) are as follows:[11,35]

- at the solid surface, the no-slip condition is applied

$$r = R_h; \quad u = 0 \tag{4}$$

- at the channel symmetry axis, the symmetry condition is used

$$r = 0; \quad \frac{\partial u}{\partial r} = 0 \tag{5}$$

- at the gas-liquid interface, velocities and normal shear stresses are coupled via the conjugate boundary conditions

$$r = R_h - \delta; \quad u_L = u_G, \quad \mu_L\frac{\partial u_L}{\partial r} = \mu_G\frac{\partial u_G}{\partial r} \tag{6}$$

Integration of Eqs. 2 and 3 and substituting the boundary conditions (Eqs. 4 – 6) yields a system of algebraic equations,[11] which is supplemented by the following flow conservation conditions

$$q_L(x) = -2\pi\int_{R_h-\delta}^{R_h} u_L(x, r)rdr = \text{const} \tag{7}$$

$$q_G(x) = 2\pi\int_0^{R_h-\delta} u_G(x, r)rdr = \text{const} \tag{8}$$

The negative sign of the lefthand side of Eq. 7 is due to the selected reference frame (see Figure 5).

The solution yields velocity profiles in the both phases *u(x,r)* together with the values of liquid film thickness along the channel height $\delta(x)$, which are used for the description of heat and mass transfer.

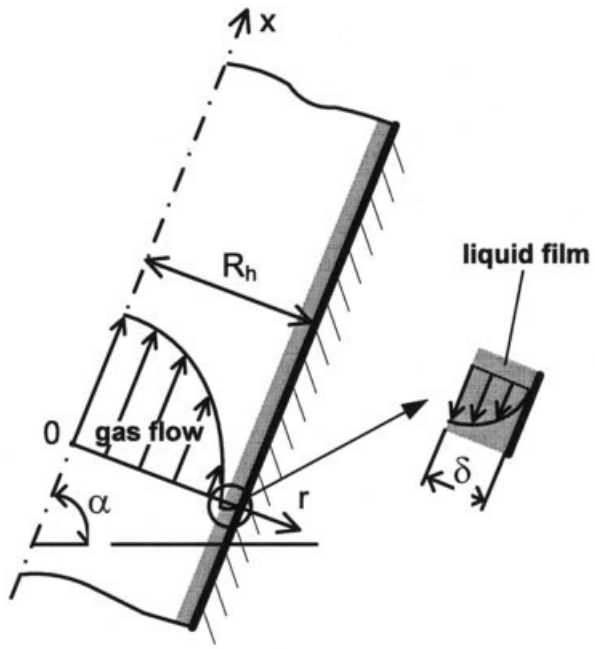

Figure 5. Two-phase countercurrent flow in a wetted channel.

Simultaneous Heat and Mass Transfer

Heat and mass transfer in each phase in a system comprising n components is described by the following transport equations

$$u(x, r)\frac{\partial T}{\partial x} = \frac{1}{r}\frac{\partial}{\partial r}\left(r\tilde{\kappa}\frac{\partial T}{\partial r}\right), \quad \tilde{\kappa} = \kappa^{lam} + \frac{\mu^{turb}}{\rho\, \mathrm{A}Pr} \tag{9}$$

$$u(x, r)\frac{\partial C_i}{\partial x} = \frac{1}{r}\frac{\partial}{\partial r}\left(r\tilde{D}_i\frac{\partial C_i}{\partial r}\right), \quad \tilde{D}_i = D_i^{lam} + \frac{\mu^{turb}}{\rho\, Sc_i}, \quad i = 1 \cdots n \tag{10}$$

where the turbulent Prandtl and Schmidt numbers Pr and Sc_i, are set equal to unity.[36]

Boundary conditions are formulated as follows:[11]

- at the entrance

$$x = 0; \quad T = T^0, \quad C_i = C_i^0, \quad i = 1 \cdots n \tag{11}$$

- at the channel wall (adiabatic and nonpermeable) and symmetry axis

$$r = R_h, \quad r = 0; \quad \frac{\partial T}{\partial r} = 0, \quad \frac{\partial C_i}{\partial r} = 0, \quad i = 1 \cdots n \tag{12}$$

- at the phase interface, concentrations and temperatures in both phases are linked via the conjugate boundary conditions (thermodynamic equilibrium, energy and mass flux continuity)

$$r = R_h - \delta; \quad T_G = T_L, \quad C_{G,i} = K_i C_{L,i}, \quad i = 1 \cdots n$$

$$\lambda_L\frac{\partial T_L}{\partial r} = \lambda_G\frac{\partial T_G}{\partial r} + \sum_{i=1}^{n}\Delta H_i D_{L,i}\frac{\partial C_{L,i}}{\partial r} \tag{13}$$

$$D_{L,i}\frac{\partial C_{L,i}}{\partial r} = D_{G,i}\frac{\partial C_{G,i}}{\partial r}, \quad i = 1 \cdots n$$

To incorporate the periodic ideal mixing (cf. Figure 4), the total channel length is subdivided into equal fragments with the lengths z_L for the liquid and z_G for the gas phase. At the entrance of each interval, the temperatures and concentrations are assigned constant values defined as integral mean temperatures and concentrations at the exit of the preceding interval. For the liquid phase, for example, the integral mean temperature is defined as

$$\bar{T}(x) = \frac{\int_{R_h-\delta}^{R_h} T(x, r)u(x, r)dr}{\int_{R_h-\delta}^{R_h} u(x, r)dr} \tag{14}$$

Equations 9 – 13 are solved numerically, using the Tri-Diagonal Matrix Algorithm.[37] For this purpose, the lefthand side of Eqs. 9 and 10, and the boundary conditions (Eq. 12) are discretized using the finite backward difference scheme, whereas for the righthand side, a second-order, central difference approximation is used. The first derivatives at the phase interface in Eq. 13 are obtained from a parabolic fit to the boundary and two inner points (second-order approximation).[38]

Numerical solution of Eqs. 9 – 13 yields local temperature and concentration fields in the both phases. These values are further used to obtain the average temperature and concentration profiles along the packing height.

Model Parameters

Geometry-related parameters

Channel Length. Length of the channels in the model presented in Figure 4 is related to the total packing height H_{pac} by the following formula

$$H = \frac{H_{pac}}{\sin\alpha} \tag{15}$$

where α represents the channel inclination angle.

Channel Diameter. Inner diameter of the channels in Figure 4 is determined as an equivalent (hydraulic) diameter of the actual channels made by the corrugated sheets (see Figure 3b). For the triangular cross-section (with one open channel side, b_0), the equivalent diameter is

$$d_h = \frac{b_0 h}{s_0} \tag{16}$$

Inclination angle. Channel inclination angle with respect to horizontal, α, is assumed to be the gravity-flow angle, in line with the experimental observations discussed above. According to Spekuljak,[22] it is a function of the corrugation geometry and the packing corrugation inclination angle. For channels with a triangular cross section, Zogg[33] proposed the following expression for the gravity-flow angle, which is adopted in our work

$$\alpha = \arctan\left(\frac{\cot\varphi}{\sin[\arctan(\cos\varphi\cot(\gamma/2))]}\right) \tag{17}$$

Channels Number. Total number of channels n_t is a function of the packing geometric specific area a_t. The volume of the packing layer shown in Figure 3a is equal to

$$V_{pac} = \frac{\pi D_{pac}^2}{4}L \tag{18}$$

Hence, a packing layer of height L and diameter D_{pac} contains a surface

$$a_{pac} = \frac{a_t\pi D_{pac}^2}{4}L \tag{19}$$

On the other hand, the total inner surface of the channels in Figure 4 is

$$a_{chn} = \frac{n_t\pi d_h}{\sin\alpha}L \tag{20}$$

Setting $a_{pac} = a_{chn}$, the total channel number is expressed as

$$n_t = \frac{a_t \sin\alpha D_{pac}^2}{4d_h} \tag{21}$$

Lengths of Undisturbed Fluid Flows. Length of the undisturbed laminar liquid flow z_L corresponds to the distance the liquid passes between the two neighboring corrugation ridges on its way over the packing surface. Given the flow angle with respect to horizontal α, the length of the undisturbed liquid flow can be estimated using the following expression[33]

$$z_L = \frac{s_0}{\tan\varphi\cos\varepsilon\sin\alpha} \tag{22}$$

where

$$\varepsilon = \arctan(\cos\varphi\cot(\gamma/2)) \tag{23}$$

For the gas flow, the length of the undisturbed interval is equal to an average channel length in a packing layer, defined as a ratio of the total channel length to their number[11]

$$z_G = \frac{\sum_{i=1}^{n} 2B_i L}{\sum_{i=1}^{n} 2(B_i\cos\varphi + L\sin\varphi) - nb_0} \tag{24}$$

Here n is a number of corrugated sheets in a packing layer,

$$n = \frac{D_{pac}}{h} \tag{25}$$

rounded off to the nearest smaller integer number, and

$$B_i = \sqrt{D_{pac}^2 - (h(n - 2(i-1)))^2}, \quad i = 1 \cdots k \tag{26}$$

is the width of ith corrugated sheet, with $k = n/2$, due to symmetrical arrangement of the corrugated sheets in a packing layer. If n is an odd number, k should be rounded-off to the nearest bigger integer, with B_k being the width of the central sheet.

Hydrodynamics-related parameters

Wetted Channels Number. Number of the wetted channels can be calculated from the packing effective specific area a_e. From Eq. 1 it follows:

$$n_w = n_t \frac{a_e}{a_t} \tag{27}$$

Determination of the packing effective specific area a_e on a purely theoretical basis represents a challenging task, due to intricate interactions between hydrodynamics and geometrical characteristics of the packing, physical properties of the system and operating conditions. Therefore, in this work, it is estimated using the following empirical correlation recently proposed by Olujić et al.[39]

$$a_e = a_e^*(1 - \Omega)\left(\frac{\sin 45^\circ}{\sin\alpha}\right)^n \tag{28}$$

Here a_e^* is defined by the well-established Onda correlation[40]

$$a_e^* = a_t\left\{1 - \exp\left[-1.45\left(\frac{0.075}{\sigma_L}\right)^{0.75}\mathrm{Re}_L^{0.1}\mathrm{Fr}_L^{-0.05}\mathrm{We}_L^{0.2}\right]\right\} \tag{29}$$

with dimensionless numbers

$$\mathrm{Re}_L = \frac{\rho_L u_{Ls}}{a_t\mu_L} \tag{30}$$

$$\mathrm{We}_L = \frac{\rho_L u_{Ls}^2}{a_t\sigma_L} \tag{31}$$

$$\mathrm{Fr}_L = \frac{u_{Ls}^2 a_t}{g} \tag{32}$$

where $u_{Ls} = 4M_L/(\rho_L\pi D_{pac}^2)$ is the liquid superficial velocity, Ω is the fraction of packing surface occupied by holes (for unperforated packings, $\Omega = 0$), n is exponent of the correction term expressed as

$$n = \left(1 - \frac{a_t}{250}\right)\left(1 - \frac{\alpha}{45}\right) + \ln\left(\frac{a_e^*}{250}\right) + \left(0.49 - \sqrt{\frac{1.013}{P}}\right)\left(1.2 - \frac{\alpha}{45}\right) \tag{33}$$

Gas-Phase Turbulent Viscosity. In this work, gas-phase turbulent viscosity in the channels with circular cross-section has been estimated using the following empirical correlation[41,42]

$$\mu_G^{turb}(r) = \rho_G R_h u_\tau \frac{\kappa}{2A}(1 - r^2)(1 + (A - 1)r^2) \tag{34}$$

Here, $u_\tau = \sqrt{|\bar{\tau}_w|/\rho_G}$ is the shear velocity, $\bar{\tau}_w$ is the shear stress at the gas-liquid phase interface, κ is the von Karman constant ($\kappa = 0.41$), and A is an empirical constant, which value is taken $A = 3.0$ according to Reichhardt.[43]

Model Verification

Verification of the suggested approach is carried out by comparing the simulated and experimental composition profiles in distillation columns operated at total reflux. Additionally, a comparison with the film model over a wide spectrum of gas loads is performed to reveal the application range and accuracy of the both modeling approaches.

Experimental data

For the verification, experimental data available in the literature are utilized. The results of pilot scale distillation tests were obtained at the University of Dortmund[44], and at the Nagoya Institute of Technology.[45]

The column in Dortmund was equipped with the Montz-Pak A3-500 gauze wire packing and had an inner diameter of 100 mm. It consisted of three sections, each 1 m high, resulting into the total packing height of 3 m. As the test systems, the binary ideal mixture chlorobenzene/ethylbenzene (CB/EB), and the ternary nonideal mixture methanol/acetonotrile/water (MeOH/ACN/WATER) were used. The tests were conducted at ambient pressure with varying feed compositions.

Widely used commercial packing Montz-Pak B1-250 was tested at the Nagoya Institute of Technology, with the methanol/ethanol/water (MeOH/EtOH/WATER) system at ambient conditions. The column had an inner diameter of 210 mm, with the total packing height of approximately 2.2 m divided into four sections. A detailed description of the experimental facilities and the sampling technique can be found elsewhere.[44,46,47]

The bed configuration employed in both these experimental studies allowed taking liquid probes along the packing height, as well as at the column top and bottom. These probes were analyzed off-line by gas chromatography.

Model Implementation

The model proposed in this article is implemented in FORTRAN. The FORTRAN routines comprise two modules, one for hydrodynamic, and one for heat and mass transport calculations. Aspen Plus® simulation engine is taken to compile the coded routines and link them to a dynamic link library (DLL-file), which can be accessed from the Aspen Plus® user interface. The main purpose of this procedure is to make the Aspen Properties® database available for calculations of the necessary physical properties. Therefore, FORTRAN coding is done in a general form, enabling any arbitrary modification of the component list without recompilation. The calculation method for the physical properties, as well as the component list can be selected using the Aspen Properties® interface. This information is stored in the Aspen Properties® problem definition files (APPDF-files) and used by referring to the databases.

As a reference model, a steady-state film model is used. It is implemented into the simulator PROFILER, created in the context of the European research project "Intelligent Column Internals for Reactive Separations (INTINT)".[48] For the estimation of model parameters, the well-established correlations elaborated at the University of Texas at Austin[3,4,16] and at the Delft University of Technology (the so-called Delft model[17,39]) are applied.

During the simulations, both the film model (PROFILER) and the model proposed in this article used the same APPDF-file for each chemical system which is necessary for an adequate comparison of the models.

The liquid-phase nonideality of the test mixtures is accounted for by the use of the UNIQUAC model.[49] The required binary interaction parameters are taken from the literature.[50]

Simulation results and discussion

Both modeling approaches use the same set of process operating parameters, namely, *flow rate*, *composition* and *temperature* of the reflux, as well as the *column top pressure,* in addition to the corrugation geometry and packing bed dimensions data, which are utilized in accordance with the individual model requirements. Liquid composition and temperature profiles calculated along the packing height are compared. Geometric characteristics of the modeled packings are summarized in Table 1. It should be noted that in the simulations, the complete surface of Montz-Pak A3-500 packing was assumed to be wetted. This assumption is appropriate for the organic mixtures. On the contrary, the application of the effective specific area correlations for the gauze wire packings proposed in Rocha et al.[4] leads to a systematic underprediction of the packing separation efficiency.

In Figures 6 and 7, a comparison of the both models with measured liquid composition profiles for different test systems and operating conditions is demonstrated for Montz-Pak A3-500 packing. F-factors given in the plots are calculated above the packing bed. Plots shown in Figure 6 compare composition profiles for the binary mixture CB/EB. Except for very small gas flow rates (see Figure 6a), agreement with experimental values is satisfactory for both hydrodynamic analogy and the film model, independently of which mass-transfer correlation is applied. It is remarkable that the hydrodynamic analogy approach reproduce the measured values especially good at low F-factors. The reason is that, under these operating conditions, assumptions of the formulated hydrodynamic analogy are very close to the real flow behavior (continuous laminar film flow of the liquid phase).

Figure 7 shows predicted and measured composition profiles for the ternary mixture MeOH/ACN/WATER. Only two components, methanol and water, are shown here in order to facilitate the presentation. Obviously, both modeling approaches are capable of predicting the compositions in the column reboiler, within the investigated F-factors range. However, when applying the film model, a proper choice of the mass-transfer correlation is crucial for the prediction accuracy. This can be well recognized in Figure 7a, in which only Bravo et al.[16] correlation yields a good agreement and Figure 7c), where both Bravo et al.[16] and Olujic et al.[39] correlations perform well. In Figure 7b, however, none of the correlations are able to predict the composition profiles throughout the packing height. The hydrodynamic analogy approach, on the contrary, exhibits a very good and stable performance for all the test studied.

Figures 8 and 9 demonstrate a comparison between the measured and predicted temperatures and compositions in the column equipped with the Montz-Pak B1-250 packing. Again, only two components, ethanol and methanol, are shown in Figure 8 to gain a clearer view. Similarly to Figures 6 and 7, nearly perfect agreement with the experimental data can be observed for the composition profiles predicted with the hy-

Table 1. Geometric Characteristics of the Modeled Structured Packings

	Montz-Pak A3-500	Montz-Pak B1-250
Layer height L, (m)	0.183	0.196
Geometric specific area a_t, (m^2/m^3)	500	247
Void fraction (−)	0.95	0.98
Corrugation angle φ, (grad)	30	45
Crimp angle γ, (grad)	74	90
Corrugation base b_0, (m)	0.009	0.0219
Corrugation side s_0, (m)	0.0075	0.016
Corrugation height h, (m)	0.006	0.011

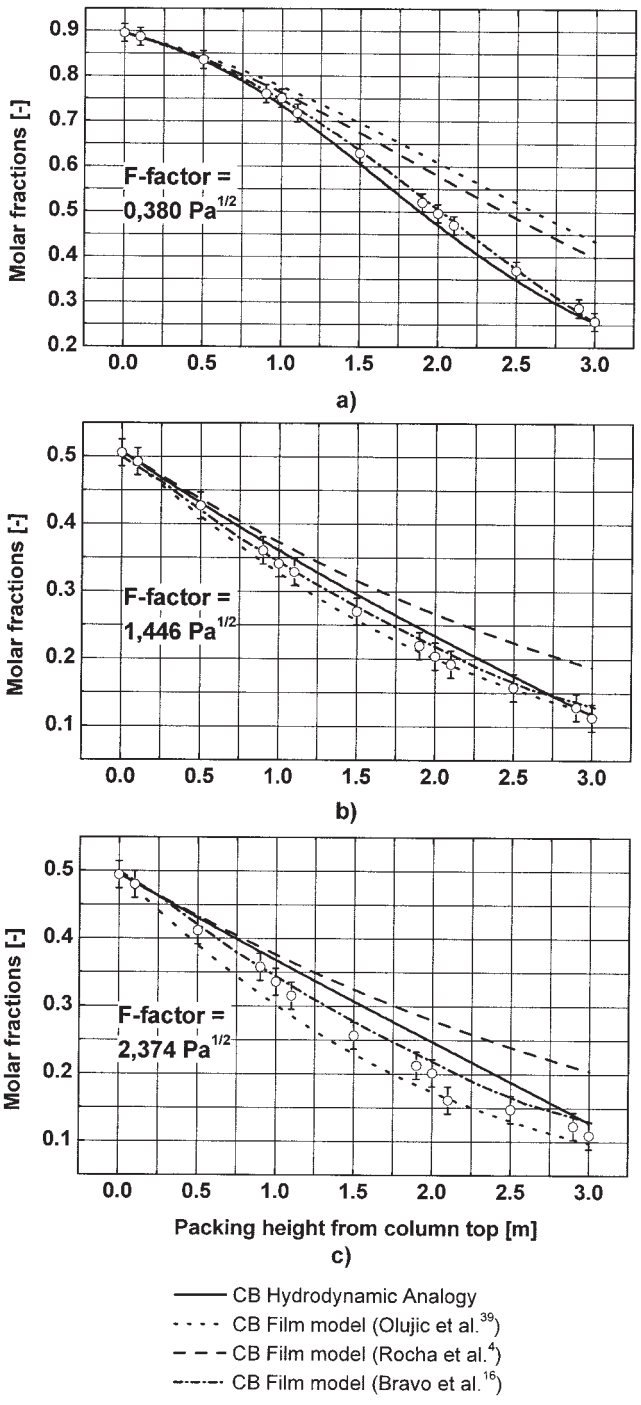

Figure 6. Predicted (lines) vs. experimental (circles) liquid composition profiles in the column with the Montz-Pak A3-500 structured packing: test mixture: chlorobenzene/ethylbenzene (CB/EB).

drodynamic analogy approach for the lower F-factors (see Figures 8a,b,c). However, for higher loads, discrepancies appear in the lower part of the column for the mixture with low-water content, Figure 8d. The discrepancies can be explained by the change in the flow conditions, namely the liquid starts to buildup in the bottom part of the column at increasing vapor flow rate. As a consequence, droplets are formed which become involved into the mass transfer, thereby, enlarging the interfacial area. The developed hydrodynamic analogy does not consider this effect, and, therefore, the discrepancy between the computed and measured compositions appears reasonable. For the water-reach mixture, however, the higher surface tension is most likely to suppress the droplets formation, resulting in the stable performance of the proposed model even for higher F-factors (cf. Figure 8e).

As it can be seen in Figures 6 to 8, the film approach provides qualitatively correct composition profiles for the both packings investigated. Obviously, the employed mass-transfer correlations were developed to maintain their validity within a

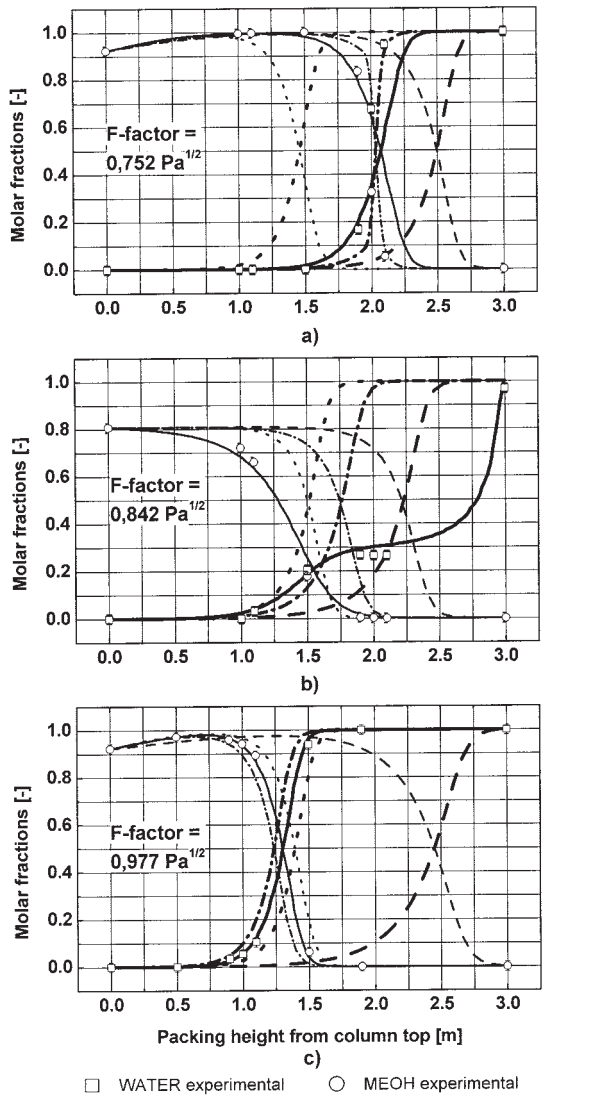

Figure 7. Predicted (lines) versus experimental (symbols) liquid composition profiles in the column with the Montz-Pak A3-500 structured packing: test mixture: ternary methanol/acetonitrile/water (MeOH/ACN/WATER).

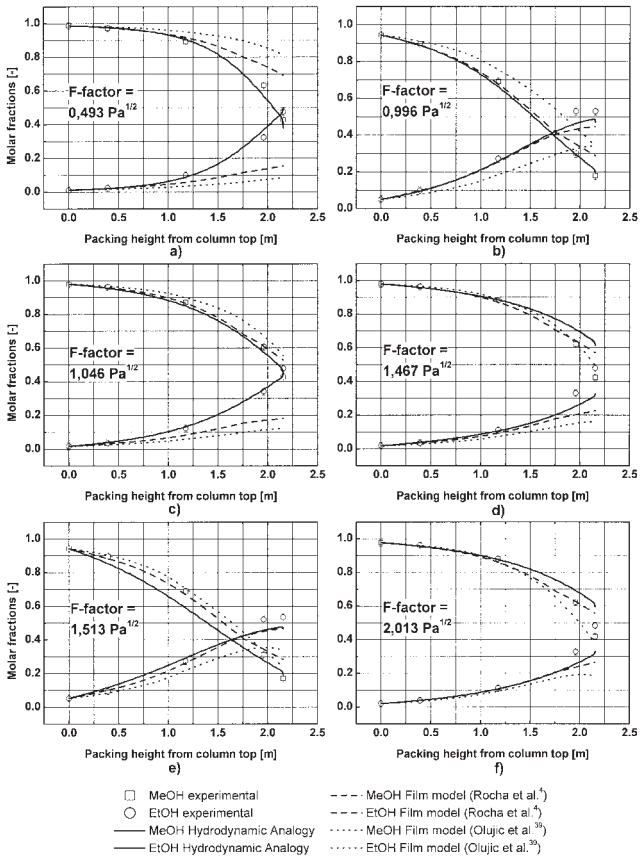

Figure 8. Predicted (lines) vs. experimental (symbols) liquid composition profiles in the column with the Montz-Pak B1-250 structured packing: test mixture: methanol/ethanol/water (MeOH/EtOH/WATER).

certain range of operating conditions near the loading point. For low-gas loads, a good agreement with experimental profiles can only be achieved with the Bravo et al.[16] correlations for the gauze wire structured packing. However, when their more recent model covering both gauze wire and metal sheet structured packings is applied (see Rocha et al.[4]), a considerable underprediction of the packings mass-transfer efficiency is evident. Similar results under these process operating conditions are obtained with the Olujic et al.[39] correlations (see Figures 6a, 7a, and 8a). It is worth noting that, contrary to the model based on hydrodynamic analogy, the accuracy of predictions with the film approach is different for different components of the multicomponent mixture. This can be explained by sensitivity of the mass-transfer correlations to the chemical systems tested.

Concluding Remarks

A model based on the hydrodynamic analogy approach has been developed for the prediction of the temperature and composition profiles in distillation columns equipped with corrugated sheet structured packings. Compared to traditional models based on the film theory, the proposed model is more rigorous. It comprises the partial differential equations governing momentum, energy and mass transport (Navier-Stokes equations, convection-diffusion and heat conduction equations) to describe the transport phenomena in an entire column. As a result, modeling the packing efficiency characteristics is accomplished without the traditional application of the transport coefficients. The direct application of the basic transport equations becomes possible because the actual complex two-phase flow in the packings is replaced by a combination of the geometrically simpler flow patterns.

In the proposed hydrodynamic analogy, the structured packing is considered as a bundle of round channels, their number and dimensions depending on the packing geometry. Liquid flows over the inner surface of some channels in accordance with the given liquid flow rate and packing wetting characteristics. The ratio of wetted channel to total channel number is defined using the correlations for the packing effective specific area. Turbulent gas flow is uniformly distributed over the whole amount of the channels occupying the rest of the volume left by the liquid flow. The gas-phase turbulence is explicitly incorporated into the model by applying an empirical correlation for the turbulent viscosity distribution in round channels. In addition, both flows are presumed to be ideally mixed at regular intervals, to account for the observed large-scale mixing due to the abrupt change of the flow directions. The lengths of these undisturbed flows represent model parameters derived from the corrugation geometry and packing layer dimensions.

It should be noted that the packing effective surface area and the gas-phase turbulent viscosity, defined here using empirical correlations, can be estimated on the basis of CFD simulations too. Specifically, a reasonable description of the turbulent viscosities as a function of F-factor and packing geometry is expected to improve the prediction accuracy for higher gas loads. Further model developments are, therefore, directed toward elimination of the above empirical correlations and introduction of the more rigorous CFD-based methods.

The system of equations to be solved comprises partial differential equations written for the gas and the liquid phases, coupled through the boundary conditions at the phase interface. Numerical solution of this system yields the local temperature and composition fields. The computed averaged compositions over the packing height are compared with measured data for distillation at total reflux for two different structured packings under a variety of operating conditions. In addition, calculations with the film model are performed, in which the necessary model parameters are estimated with the well-established correlations developed at the University of Texas and at the Delft

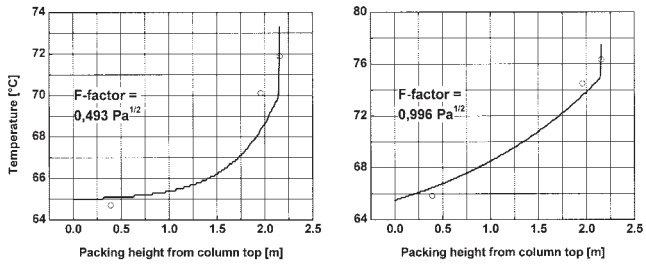

Figure 9. Example of predicted (solid line) and experimental (circles) temperature profiles in the column with the Montz-Pak B1-250 structured packing: test mixture: methanol/ethanol/water (MeOH/EtOH/WATER).

University of Technology. The main purpose of this comparison is to evaluate prediction accuracy of the traditional and the novel modeling approaches.

The accuracy of the film model strongly depends on the applied correlations, chemical systems and operating conditions. On the contrary, the model based on the hydrodynamic analogy approach demonstrates a stable performance with all tested systems and over a broad range of investigated F-factors. Also a better agreement with experiment is observed for the both packings. Some deviations appear only in the lower part of the metal sheet structured packing bed for the mixture with the low water content, when the flow conditions close to the loading point are considered. These deviations are attributed to the change in the flow regime, which is not considered in the model developed.

The proposed approach is more rigorous and physically consistent than the traditional film model. It demonstrates an excellent agreement with experimental data and can be recommended for design, revamp and optimization of (reactive) distillation columns equipped with the corrugated sheet structured packings.

Acknowledgments

The financial support provided by the foundations "Stiftung Stipendien-Fonds des Verbandes der Chemischen Industrie e.V." and "Herbert Quandt-Stiftung der VARTA AG" is greatly acknowledged.

Notation

a_e = packing effective specific area, m^2 / m^3
a_{pac} = surface contained in a single packing layer, m^2
a_{chn} = inner surface area of channels corresponding to a packing layer, m^2
a_t = packing geometric specific area, m^2 /m^3
B = width of a single corrugated sheet, m
b_0 = corrugation base, m
C = molar concentration of a component, kmol / m^3
D = binary diffusivity of a component, m^2 / s
$\tilde{D}$ = effective binary diffusivity of a component defined by Eq. 10, m^2/s
d_h = channel hydraulic diameter, m
D_{pac} = packing layer diameter, m
Fr = Froude number defined by Eq. 32
g = acceleration of gravity, m / s^2
H = channel height, m
ΔH = vaporization enthalpy of a component, J/kmol
h = corrugation height, m
K = phase equilibrium constant of a component
L = packing layer height, m
M = mass flow rate, kg / s
n_t = total number of channels
n_w = number of wetted channels
P = pressure, Pa
Pr = Prandtl number, $\mu/(\rho\kappa)$
q = volumetric flow rate in a single channel, m^3 / s
R_h = channel hydraulic radius, m
Re = Reynolds number defined by Eq. 30
s_0 = corrugation side, m
Sc = Schmidt number, $\mu/(\rho D)$
T = local temperature, K
$\bar{T}$ = average temperature, K
u = local velocity, m / s
u_τ = shear velocity, m / s
V_{pac} = packing layer volume, m^3
We = Weber number defined by Eq. 31
z = length of undisturbed fluid flow, m

Greek letters

α = gravity-flow angle, grad
γ = crimp angle, grad
δ = liquid film thickness, m
ε = angle defined by Eq. 23, grad
κ = thermal diffusivity, m^2 / s
$\tilde{\kappa}$ = effective thermal diffusivity defined by Eq. 9, m^2 / s
λ = thermal conductivity, J / (msK)
μ = molecular viscosity, Pa s
$\tilde{\mu}$ = effective viscosity defined by Eq. 3, Pa s
ρ = mass density, kg / m^3
σ = surface tension, N / m
φ = corrugations inclination angle (with respect to column axis), grad
Ω = fraction of packing surface occupied by holes

Subscripts and Superscripts

0 = initial value
G = gas or vapor phase
L = liquid phase
Ls = liquid superficial velocity
lam = laminar flow
turb = turbulent flow

Literature Cited

1. Spiegel L, Meier W. Distillation columns with structured packings in the next decade. *Trans IChemE.* 2003;81:39-47.
2. Kurtz DP, McNulty KJ, Morgan RD. Stretch the capacity of high-pressure distillation columns. *Chem Eng Prog.* 1991;87:43-49.
3. Rocha JA, Bravo JL, Fair JR. Distillation columns containing structured packings: A comprehensive model for their performance. 1. hydraulic models. *Ind Eng Chem Res*. 1993;32:641-651.
4. Rocha JA, Bravo JL, Fair JR. Distillation columns containing structured packings: A comprehensive model for their performance. 2. Mass-transfer model. *Ind Eng Chem Res*. 1996;35:1660-1667.
5. Fitz CW, Kunesh JG, Shariat A. Performance of structured packing in a commercial-scale column at pressures of 0.02-27.6 bar. *Ind Eng Chem Res*. 1999;38:512-518.
6. Olujic Z, Seibert AF, Fair JR. Influence of corrugation geometry on the performance of structured packings: An experimetal study. *Chem Eng Process*. 2000;39:335-342.
7. Casey M, Lang E, Mack R, Schlegel R, Wehrli M. *Applications of Computational Fluid Dynamics for Process Engineering at Sulzer*. Speedup 12; 1998.
8. Billingham JF, Lockett MJ. Development of a new generation of structured packings for distillation. *Chem Eng Res Des.* 1999;77:583-587.
9. Kessler A, Moser F, Meier W. MellapakPlus: *A New Generation of Structured Packings*. AIChE Annual Meeting; 1999.
10. Brunazzi E, Paglianti A. Mechanistic pressure drop model for columns containing structured packings. *AIChE J*. 1997;43:317-327.
11. Shilkin A, Kenig EY. A new approach to fluid separation modelling in the columns equipped with structured packings. *Chem Eng J*. 2005; 110:87-100.
12. Lewis WK, Whitman WG. Principles of gas absorption. *Ind Eng Chem*. 1924;16:1215-1220.
13. Kenig EY, Gorak A, Pyhälanti A, Jakobsson K, Aittamaa J, Sundmacher K. Advanced rate-based simulation tool for reactive distillation. *AIChE J*. 2004;50:322-342.
14. Hirschfelder JO, Curtiss CF, Bird RB. *Molecular Theory of Gases and Liquids*. New York: Wiley; 1964.
15. Stewart WE, Prober R. Matrix calculation of multicomponent mass transfer in isotermal systems. *Ind End Chem Fund*. 1964;3:224-235.
16. Bravo JL, Rocha JA, Fair JR. Mass transfer in gauze packing. *Hydrocarb Process*. 1985:91-95.
17. Olujic Z. Development of a complete simulation model for predicting the hydraulic and separation performance of distillation columns equipped with structured packings. *Chem Biochem Eng Q*. 1997;11: 31-46.
18. Aroonwilas A, Chama A, Tontiwachwuthikul P, Veawab A. Mathematical modelling of mass-transfer and hydrodynamics in co_2 absorbers packed with structured packings. *Chem Eng Sci*. 2003;58:4037-4053.
19. Kenig EY. Multicomponent multiphase film-like systems: A modeling approach. *Comput Chem Eng*. 1997;21:S355–S360.

20. Bird RB, Stewart WE, Lightfoot EN. *Transport Phenomena.* 2nd ed. John Whiley & Sons, Inc; 2002.
21. van Baten JM, Ellenberger J, Krishna R. Radial and axial dispersion of the liquid phase within a KATAPAK-S structure: experiments vs. CFD simulations. *Chem Eng Sci*. 2001;56:813-821.
22. Spekuljak Z. Modelacion de Rellenos Regullares de Alta Eficienca Para la Transferencia de Materia, Universidad Nacional del Litoral; 1986. PhD thesis.
23. Zhao L, Cerro RL. Experimental characterization of viscous film flows over complex surfaces. *Int J Multiphase Flow*. 1992;18:495-516.
24. Stoter F. *Modelling of Maldistribution in Structured Packings: From Detail to Column Design*. Delft University of Technology, 1993. PhD thesis.
25. Valluri P, Matar OK, Hewitt GF, Mendes MA. Thin film flow over structured packings at moderate reynolds numbers. *Chem Eng Sci*. 2005;60:1965-1975.
26. Shetty S, Cerro RL. Fundamental liquid flow correlations for the computation of design parameters for ordered packings. *Ind End Chem Res*. 1997;36:771-783.
27. Zogg M. Strömungs- und Stoffaustauschuntersuchungen an der Sulzer-Gewebepackung, Technische Hochschule Zürich; 1972. PhD thesis.
28. Petre CF, Larachi F, Iliuta I, Grandjean BPA. Pressure drop through structured packings: breakdown into the contributing mechanisms by CFD modeling. *Chem Eng Sci.* 2003;58:163-177.
29. Egorov Y, Menter F, Kloeker M, Kenig EY. On the combination of CFD and rate-based modelling in the simulation of reactive separation processes. Chem. Eng. Process. 2005;44:631-644.
30. Joshi JB, Ranade VV. Computational fluid dynamics for designing process equipment: expectations, current status, and path forward. *Ind Eng Chem Res*. 2003;42:1115-1128.
31. Olujic Z, Jansen H, Kaibel B, Rietfort T, Zich E. Stretching the capacity of structured packings. *Ind Eng Chem Res*. 2001;40:6172-6180.
32. Behrens M, Saraber PP, Jansen H, Olujic Z. Performance Characteristics of a Monolith-Like Structured Packing. Chem. Biochem. Eng. Q. 2001;15:49-57.
33. Zogg M. Modifizierte Stoffübergangskoeffizienten für bilanzmäßige Stoffübergangsberechnungen an laminaren Rieselfilmen. *Chem Ing Tech*. 1972;44:930-936.
34. Levich G. Physicochemical Hydrodynamics. New Jersey: Prentice Hall, Englewood Cliffs; 1962.
35. Kholpanov LP, Avetisyan KV, Malysov VA. Fluid mechanics and mass transfer during three-phase membrane extraction. *Theor Found Chem Eng*. 1988;22:299-305.
36. Reynolds AJ. *Turbulent Flows in Engineering*. London: Wiley; 1974.
37. Patankar SV. *Numerical Heat Transfer and Fluid Flow*. Hemisphere Publ. Corp., New-York: McGraw Hill; 1980.
38. Ferziger JH, Peric M. *Computational Methods for Fluid Dynamics*. 3rd ed. Berlin: Springer-Verlag; 2002.
39. Olujic Z, Behrens M, Colli L, Paglianti A. Predicting the Efficiency of Corrugated Sheet Structured Packings with Large Specific Surface Area. Chem. Biochem. Eng. Q. 2004;18:89-96.
40. Onda K, Takeuchi H, Okumoto Y. Mass Transfer Coefficients Between Gas and Liquid Phases in Packed Columns. *J Chem Eng Japan*. 1968;1:56-62.
41. Gersten K, Herwig H. Strömungsmechanik. Grundlagen der Impuls-, Wärme- und Stoffübertragung aus asymptotischer Sicht. Wiesbaden: Vieweg; 1992.
42. Schlichting H, Gersten K. *Grenzschicht-Theorie*. Berlin: Springer; 1997.
43. Reichhardt H. Vollständige Darstellung der turbulenten Geschwindigkeitsverteilung in glatten Leitungen. Z. angew. *Math Mech* 1951;31: 208-219.
44. Pelkonen S, Gorak A, Ohligschläger A, Kaesemann R. Experimental study on multicomponent distillation in packed columns. *Chem Eng Process*. 2001;40:235-243.
45. Mori H, Ibuki R, Taguchi K, Futamura K, Olujic Z. Three-component distillation using structured packings: Performance evaluation and model validation. *Chem Eng Sci*. 2006;61:1760-1766.
46. Mori H, Oda A, Kunimoto Y, Aragaki T. Packed column distillation simulation with a rate-based method. *J Chem Eng Japan*. 1996;29: 307-314.
47. Pelkonen S. Multicomponent mass transfer in packed distillation columns. University of Dortmund, 1997. PhD thesis.
48. Kloeker M, Kenig EY, Hoffmann A, Kreis P, Gorak A. Rate-based modelling and simulation of reactive separations in gas/vapour-liquid systems. *Chem Eng Process*. 2005;44:617-629.
49. Hartmann K, Schirmer W, Slinko MG. Modellierung von Phasengleichgewichten. Berlin: Akademie-Verlag; 1981.
50. *Vapor-Liquid Equilibrium Data Collection*. DECHEMA Chemistry Data Series.

Manuscript received Nov. 14, 2005, and revision received Jun 6, 2006.